Vol. 37, No. 1 (2015) 42-54

Tribology in Industry

www.tribology.fink.rs

RESEARCH

Finite Element Analysis for Coating Strength of a Piston Compression Ring in Contact with Cylinder Liner: A Tribodynamic Analysis

P.C. Mishra[a], Prakhardeep[a], S. Bhattacharya[a], P. Pandey[a]

[a] *Green Engine Technology Center, School of Mechanical Engineering, KIIT University, Bhubaneswar, India.*

Keywords:

Compression ring
Cylinder liner
Finite element method
Coating
Von Misses Stess-strain
Deformation

†Corresponding author:

Prakash Chandra Mishra
Green Engine Technology Center,
School of Mechanical Engineering,
KIIT University ,Bhubaneswar, India
E-mail: pmishrafme@kiit.ac.in

A B S T R A C T

Piston Compression ring is the constituent part of ring-liner sliding pair that is subjected to high load and speed condition. Due to lubrication regime transition, there is the greater chance of wear and tear in the ring as well as in the liner. In order to reduce the wear and to enhance the ring and liner life, ceramic coatings are provided on the surface of such contact pairs. Current paper uses a finite element method to analyze the coating strength of a compression ring at compression and power stroke transition, where peak combustion pressure is higher than other crank positions. The deformation, von Misses stress and strain in the core and coating interface are discussed elaborately.

1. INTRODUCTION

Recent research predicts more than 70 % of energy used in an IC engine is in some form of losses. Engine emission cooling and friction are the measure cause of losses in an IC engine which reduce its efficiency. However, friction loss happens due to the errant dynamics of the engine subsystems that includes piston assembly, engine bearings, valves and timing gears. Piston subsystem is the major contributor of friction loss that accounts more that 80 % of Mechanical losses in an engine [1].

Piston assembly consists of the piston rings mounted on the groove of the piston body. While it is in motion, there are many contacting surfaces subjected to sliding with reasonable loads and speeds. Such a simultaneous action of sliding and reciprocation leads to the wear and tear of the ring, liner and piston. Thermal and wear resistant coatings of few nano to micro meter depth are coated on the surface of piston subsystem components that reduce wear and enhance the component life [5]. The coating is done by physical and chemical vapour deposition technique which provides a protective layer to the component and possesses the same strength as the core component material [6] .

Coating strength of a material can be estimated by considering the ring dynamic behaviour, lubricant strength, engine speed, combustion gas pressure and the coating material bonding strength etc. [1,2]. Kubert and Kumar [3] carried out a finite element method (FEM) simulation of the piston ring in a multi-body single cylinder internal combustion engine. The model deals with an assembly of piston top compression ring, liner, connecting rod and the crank shaft. The results of such simulation show that the engine performance was influenced by the ring geometry, coating, method of coating and the mechanical and thermal properties. Through this research, the ring deformation and stresses developed in the ring-liner interface were evaluated using FEM.

Dunaevsky et al. [4] studied the three dimensional distortion of the piston ring in an arbitrary cross-section to understand its importance on oil flow and blow-by. The modal distortion of piston ring occurs either due to installation stresses or due to operational parameters like gas pressure, friction and thermal load. The model was applied to several typical cross-sections. A comprehensive three dimensional theory of piston ring installation and distortion was developed through this research. Further, the piston ring conformability was aimed through various engineering optimisation with the consideration of both Young's and shear Moduli. Along with this, a model of conformability analysis of a split piston ring with arbitrary cross-section was developed with consideration of bore profile and centre-line of piston ring through Fourier harmonics.

Method of coating requires a sound knowledge of core and coating materials. Minewitsch [5] studied some developments of triboanalysis methods for the coated machine components. Various sliding and rolling pairs and the appropriate coating material requirement for each case are discussed through this research. The depth of coating and the method of coating and its influence on the coated component tribological performance is also studied. This literature gives a fundamental charecterstics of coating and coated component performance.

Nano composites are widely used for surface coating applications. Urgeon [6] studied the tribological properties of nano composite coating like MeN-X (for example nano sized MoN) that is surrounded by Cu, Ag or Sn like soft materials. This combination of coating and substrate exhibits high hardness to sustain up to 40 GPa of asperity contact pressure. It has less friction coefficient and negligible wear against steel, aluminium and alumina.

To understand the coating strength, it is essential to understand the contact pressure of the ring on bore surface due to its elasticity. Okamoto and Sakai [7] studied the contact pressure distribution around an incomplete circular piston ring using elementary theories and problems by Timoshenko [8]. They correlated the ring material strength and the ring curvature with global deflection of the ring while in-situ. The friction loss and the wear are more significant in compression and power stroke transition. Such transient crank location is known as the high pressure zone of an engine cycle [9,17,18]. The mixed regime prevails there due to more outward springing action. The elastohydrodynamic action on the coating is obvious.Hence, Hallavacek [10] derived the formula for the central film thickness between cylinder liner and soft incompressible coated piston ring taking concept of elastohydrodynamic lubrication. Further to such analysis Tanaka et al. [11] used ceramic-metal composite coated piston ring and cylinder of low speed marine diesel engine. Funatani and Kurosawa [12] verified the improvement in performance of Nickel and Ceramic composite as coating material.

Kennedy et al. [13] experimented the fact that coating in piston ring of gasoline engine reduces friction to significant extent. Further, Tung and Mc Millan [14] over view the tribology of automotive contacting components and stated the need of coating in reducing engine friction. Bouzakis [15] et al. studied the temperature and nano indentation resistance of PVD coated components and simulated the same using finite element method. There are many such theoretical and experimental researches reported in the past regarding the benefits of coating in enhancing contacting component life.

Barrel et al. [16] carried out simulated experiments for impact and sliding wear in top piston ring groove of a gasoline engine. The influence of normal impact and sliding wear and

surface damage at lubricated interface between the top piston ring and the bore was investigated using a specially adapted tribometer. Standard production components were tested and the piston ring used was nitro-carborised with a production lap finish. The piston was a hyper-eutectic aluminium-silicon alloy, either tin plated or hard ionised. Experiments were performed at various loads, velocities and temperatures comparable to a modern automobile engine of four stroke and gasoline type under both dry condition and with fully formulated SAE 10W30 engine oil. Lubricant starvation was found to be the most critical operational parameter leading to surface damage and wear. An important phenomenon observed was tendency of piston material to transfer and adhere to the ring surface. This phenomenon is called micro-welding. Anodizing was shown to a very effective treatment to resist micro- welding.

Based on this literature information, it is understood that coating is a useful technique to improve tribological performance of relatively moving components. Therefore, finite element model for coating strength analysis of piston ring considering the forces generated due to sliding motion could be worth studying the coating life.

2. THEORY OF MODEL

Piston compression ring of a running engine is subjected to many forces. Those include combustion pressure force, ring elastic pressure force and lubrication reaction force. All these forces together governs the ring modal behavior and contact wear. Hence it is necessary to compute all these forces before the finite element analysis of coating strength.

2.1 Piston ring dynamics and tribology

Piston rings together contribute more than 80% engine friction loss [9]. The compression ring is most friction contributing ring due to its simultaneous sealing, cleaning and lubricating action. It is an incomplete circular ring and is mounted on the piston ring groove. Then it is squeezed into the cylinder bore such that an inherent outward springing action will be offered by it to the liner after installation as well as in the engine operation.

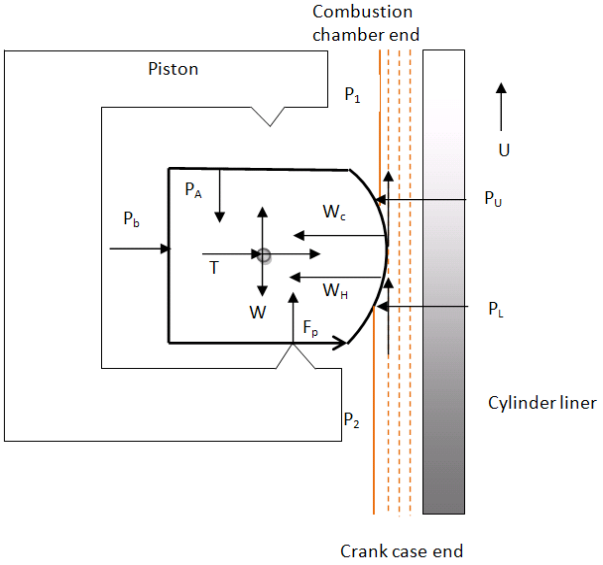

Fig. 1(a). Force components in a dynamic piston ring.

The three dimensional (3-D) modal behavior of the ring is governed by combustion gas pressure, ring elasticity, lubricant reaction and the changeable support as shown in the Fig. 1(a). Due to the simultaneous action of these forces acting on the ring, 3-D modal behaviors such as radial outward deformation, axial tilt, out of plane bending and tilting are executed. As a result of which, the ring is in contact with the groove land in more contact area and suffer less deformation or stress on the interface of the coating and substrate.

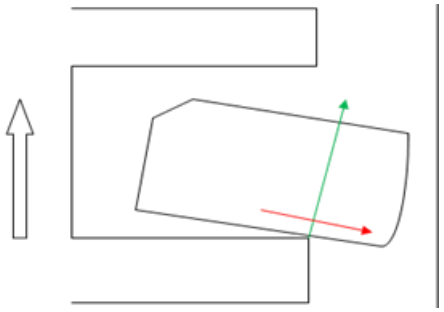

Fig. 1(b). Piston upward motion (compression and exhaust stroke).

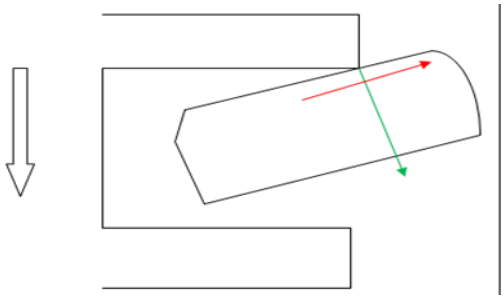

Fig. 1(c) Piston downward motion (power and suction stroke).

But if this contact is because of tilting as shown in the Figs. 1(b) and 1(c), the real contact area of groove and ring is very less. Therefore, the highly localized stress developed in the ring causes the coating failure and severe ring wear.
The forces, which are acting simultaneously on the ring in both these cases include:

- Total axial friction force per unit circumference (F) owing to hydrodynamic action and asperity contact.
- Radial friction force per unit circumference at pivot.
- Gas pressure above (P_1) and below the ring (P_2).
- Axial Gas pressure force (P_r) per unit circumference.
- Radial gas pressure force (P_b) due to gas pressure acting radial to the back of the ring.
- Axial component of hydrodynamic force (R_H) per unit circumference.
- Axial reaction force per unit circumference (F_p) at pivot.
- Radial force per unit circumference (W_c) owing to asperity contact.
- Radial component of hydrodynamic force (W_h).
- (T) radial force per unit circumference owing to inherent ring elastic tension.

All these forces are generated due to three basic forces such as the combustion gas pressure force, ring elastic pressure force and the lubricant reaction pressure/film pressure force. Those initiated due to the combustion of air fuel mixture, inherent ring elasticity and piston sliding motion in lubricated contact with ring respectively.

2.1.1 Combustion gas pressure

The gas pressure due to combustion is created because of the explosive burning of air fuel mixture after ignition. As given in the Fig. 2, the gas pressure up to 120 bars is generated during the engine cycle. During the upward motion of the piston, the gap between ring and the groove land exposed to direct combustion pressure and create more outward sealing action in the ring. But during downward motion such back pressure in the ring is ceased due to absence of gap resulting different force configuration.

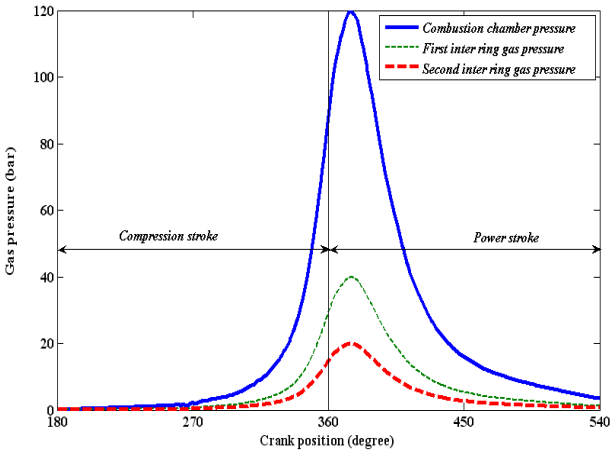

Fig. 2. Cyclic variation of Gas pressure and inter ring gas pressure.

2.1.2 Elastic pressure

Elastic pressure is exerted by the installed ring on the cylinder liner due to the outward springing action. It tries to conform on the bore surface during installation as well as during running. In a running engine during piston upward motion, more conformances achieved due to combustion chamber pressure. The radial displacement (global in-plane deflection) $\Delta_{i,j}$ as given in the Fig. 3, at any position i due to the application of radial force Q_j at position j is, thus, given in the equation (1) as:

$$\Delta(i,j)=\frac{r_0^3}{EI}a_{ij}Q_j \tag{1}$$

The induced elastic pressure in the ring due to this deformation is:

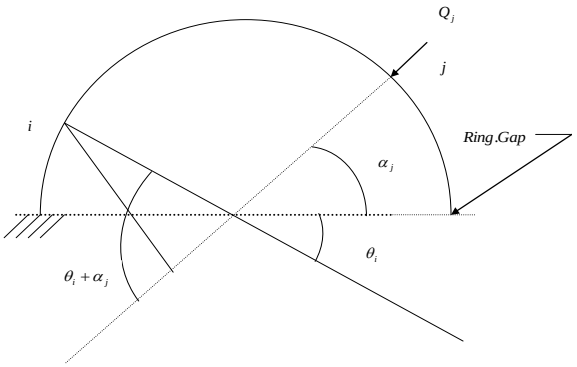

Fig. 3. Position of force and deformation in general approach.

$$P_{eij}=\frac{EI}{2\pi a_{i,j}br_0^4}\Delta_{i,j} \tag{2}$$

where:

$$f(\theta_i,\alpha_j)=\begin{Bmatrix}\cos\alpha_j\sin\theta_i\left(\frac{1}{2}\sin^2\theta_i\right)+\cos\alpha_j\sin\theta_i\left(\frac{1}{4}\sin 2\theta_i+\frac{\theta_i}{2}\right)\\ -\cos\alpha_j\cos\theta_i\left(\frac{\theta_i}{2}-\frac{1}{4}\sin 2\theta_i\right)-\sin\alpha_j\cos\theta_i\left(\frac{1}{2}\sin^2\theta_i\right)\end{Bmatrix} \quad (3)$$

Therefore, the elastic force acting outward on the ring is:

$$W_{elastic}=\sum\sum P_{e_{ij}}dxdy \quad (4)$$

The deflection can be calculated experimentally as show in the Fig. 4 and the elastic pressure developed after the mounting of the ring can be estimated using equation (2).

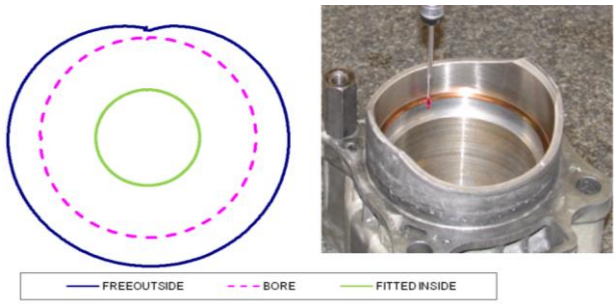

Fig. 4. Measurement of ring and bore circumference.

As the maximum ring elastic pressure is of order 0.22 MPa and the variation is (0-0.2) MPa. It is considered that the elastic pressure of 0.2 Mpa uniform throughout the ring circumference is applied in entire engine cycle. During compression and power stroke transition (300^0-400^0) degree crank angle (C.A.), the back pressure due to combustion gas remains dominant, which is in order of 12 MPa (in case high torque and high speed engine). Hence, it is necessary to study the ring-bore conformability of a running engine in detail.

2.1.3 Conformability analysis

The bore out of roundness can be mathematically quantified with the help of Fourier series as given in equation (5).

$$\Delta R(\theta)=\sum_{i=2}^{n}\left(A_i\cos i\theta+B_i\sin i\theta\right) \quad (5)$$

A_i & B_i are the Fourier coefficients at position i with maximum order n. Conformability is the ability of ring to conform in the out-of-round bore. For an nth order bore, the mathematical formulation of conformability factor is given as per Mishra [9] in equation (6) as:

$$\xi_n(\theta)=\frac{3\left[F_e+F_g(\theta)\right]R_b^2(D-a)^2}{Eba^3\left(n^2-1\right)^2} \quad (6)$$

Where, F_e is the elastic force due to ring tension, F_g (θ) is the net gas pressure force, R_b is the nominal bore radius, D is nominal bore diameter, E is modulus of elasticity of the ring, b is ring depth and a is ring axial width. The lubricant reaction force causes due to sliding action of piston. It gives rise to elastohydrodynamics of ring-liner contact. The hydrodynamic pressure and also the reaction force developed due to lubricated contact influence the coating strength. Hence, the mechanism of its development should be discussed in more detail.

2.1.4 Transient elastohydrodynamics of ring liner lubrication

Lubricant performs to avoid the contact of relatively moving parts because it's viscous property and incompressibility. When it passes through the converging and diverging gap of mating surfaces, the hydrodynamic pressure is developed and provides the cousin effect and maintains separation. Such pressure determines the load bearing ability, friction force, and flow-in to the conjunction. In order to obtain such pressure we have solved the Reynolds equation as given in equation (7).

$$\begin{Bmatrix}\frac{\partial}{\partial x}\left(\phi_p\frac{h^3}{12\eta}\frac{\partial P_h}{\partial x}\right)+\frac{\partial}{\partial y}\left(\phi_p\frac{h^3}{12\eta}\frac{\partial P_h}{\partial y}\right)\\ =\frac{U}{2}\frac{\partial\left(\phi_g h\right)}{\partial x}+\frac{U}{2}\lambda_k\frac{\partial\phi_s}{\partial x}+\frac{\partial h}{\partial t}\end{Bmatrix} \quad (7)$$

The lubricant in running state of the engine is subjected to piezo-viscous behavior change. It is based on the formulation given in equation (8).

$$\eta=\eta_0\exp^{(\ln\eta_0+9.67)\left(-1+\left(1+5.1\times10^{-9}P_h\right)\right)} \quad (8)$$

The roughness parameter in this case is measured and presented in Fig. 5.

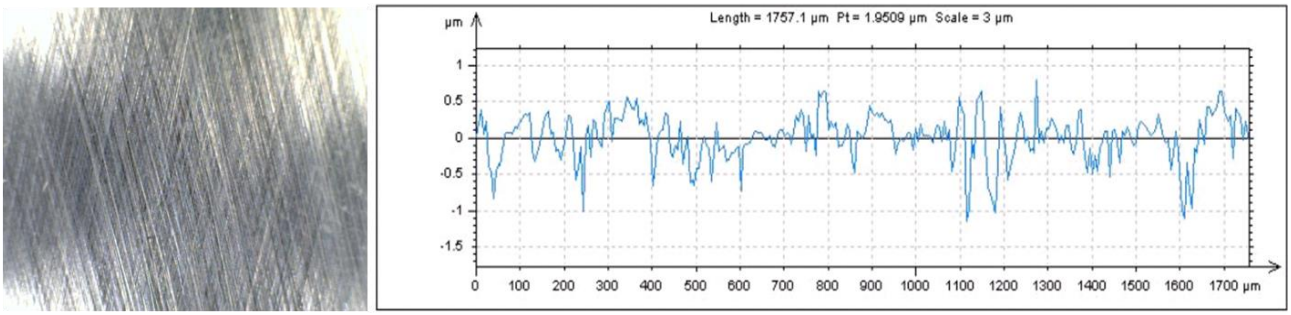

Fig. 5. Measured roughness of cross h patterned cylinder liner.

2.1.5 Method of EHL solution and Boundary conditions

The finite difference method based numerical computation is used along with the low relaxation effective influence Newton-Raphson method with appropriate pressure convergence (given in equation (9), and with Reynolds/Swift-Steiber exit boundary condition. The load convergence is carried out together with film relaxation to find the appropriate gap, using a suitable damping factor (given in equation (10)).

$$Error^{p_h} = \frac{\sum_{i}^{n}\sum_{j}^{m}\left|P_{hi,j}^{K+1} - P_{hi,j}^{K}\right|}{\sum_{i}^{n}\sum_{j}^{m}\left|P_{hi,j}^{K+1}\right|} \le 0.01 \qquad (9)$$

Where, $error^{p}$ is the error of pressure K convergence, is the number of iteration step, (i, j) is position vector.

$$h_0(\theta)^k = h_0(\theta)^{k-1} - \left\{\vartheta\left|\frac{F_{ap} - W}{F_{ap}}\right|\right\} \qquad (10)$$

Where, $h_0(\theta)$ is the minimum film thickness, $F_{ap}(F_g + F_e)$ is the applied external force and W is the estimated lubricant reaction force. Through this iterative method the film is made exact for the corresponding applied force.

For the sake of computation, the entire contact area is unwrapped to a rectangular dimension of (200 x 180). Therefore, 200 nodes are taken into the axial direction of the ring and 180 nodes are taken along the ring circumference. At every crank location the numerical boundary for pressure is set as: p(1,1) = 0, p(1,j) = 0, p(i,1) = 0 and p(200,180) = 0. Also, for any negative pressure before rupture point is set to zero. The pressure after rupture point is set to zero due to non-consideration of cavitation. The rupture point is at the middle of the ring axial width. The direction of sliding motion is *x*. Thus, the instantaneous speed of entraining motion of the lubricant into the conjunction is: $U = \dot{x}$ ($\dot{x}$ being the sliding velocity of the ring relative to the stationary liner), $V = 0$ (no side-leakage of lubricant in the circumferential contact direction is assumed).

2.1.6 Asperity contact force

With an insufficient film of lubricant, the asperity interactions occur between any pair of rough surfaces in close contiguity. Greenwood and Tripp [17] proposed a model to obtain the pressure distribution between two rough surfaces with normally distributed asperity heights:

$$p_{asp} = K^{*}E^{'}F_{2.5}(\lambda_{rk}) \qquad (11)$$

The surface roughness of both the ring and the bore are assumed to be isotropic. The function $F_{2.5}(\lambda_{rk})$ relates to the probability distribution of asperity heights. For a Gaussian distribution of asperities, $F_{2.5}(\lambda_{rk})$ has the following form:

$$F_{2.5}(\lambda_{rk}) = \frac{1}{\sqrt{2\pi}}\int_{\lambda_{rk}}^{\infty}(s - \lambda_{rk})^{5/2} e^{\frac{s^2}{2}} ds \qquad (12)$$

A curve-fit of the function is more suited to numerical analysis. For typical ring-bore contact Hu *et al* [18] state that:

$$F_{2.5}(\lambda_{rk}) = \begin{cases} A(\beta^{*} - \lambda_{rk})^{z} & \lambda_{rk} \le \beta^{*} \\ 0 & \lambda_{rk} > \beta^{*} \end{cases} \qquad (13)$$

where: $\beta^{*} = 4$, $A = 4.4068\times10^{-5}$, $z = 6.804$, and $\lambda_{rk} = \frac{h}{\sigma_{rms}}$ (Stribeck's oil film parameter).

K^* in equation (11) is a function of the surface roughness as:

$$K^* = 5.318748 \times 10^{10} \sigma_{rk}^{5/2}.$$

The generated contact pressures are due to viscous action of the fluid (hydrodynamic/elastohydrodynamic) and the asperity contact pressures. At any instant of time in the engine cycle, the applied force acting on the ring-bore conjunction is obtained as:

$$F = F_e + F_g \tag{14}$$

$$W = \int\int p dx dy \tag{15}$$

where: $p = p_h + p_{asp}$.

2.1.7 Friction Force in mixed regime

Due to rapid shear of lubricant layer, there occurs the fluid friction. It is the integration of shear stress that is developed (given in Eq. (17)) in the conjuction. The expression for shear stress is as per Eq. (16). The shear stress developed in mixed regime is as:

$$\tau = \frac{\eta U}{h}\left(\phi_{fg} + \phi_{fs}\right) - \phi_{fp}\frac{h}{2}\frac{\partial p}{\partial x} \tag{16}$$

Hence, the friction force is the integration of the shear stress over the contact area and is:

$$F = \iint \tau dx dy \tag{17}$$

It means the total shear in the contact is equal to the sum of the shear in the fluid film region and that in the cavitation region. The Fig. 6 represents all the forces acting on a piston ring at highest gas pressure (120 bars in this case).

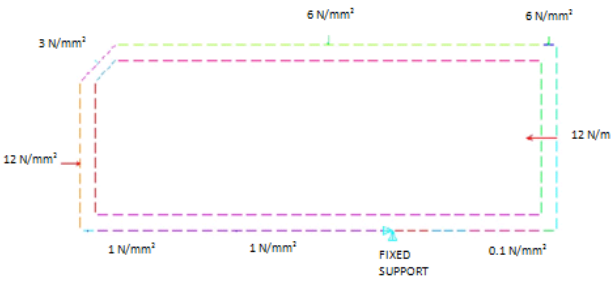

Fig. 6. Components of estimated forces in a piston ring.

2.2 Finite element method of coated piston ring

Based on the forces applied, the interface of piston ring and the coating layer develops stress, the maximum value of which is at the point of contact at the groove land. Due to development of such stress and further due to frequent loading and unloading at contact point, the failure occurs in the coating, as a result of fatigue.

2.2.1 CAD Modelling of Piston ring

Prior to doing the finite element modelling of piston ring, the geometry of the same need to be prepared using any computer aided draft tools. In this paper, the CATIA V5R19 is used for drafting of three dimensional ring. The Fig. 7 represents the CAD model of coated piston ring.

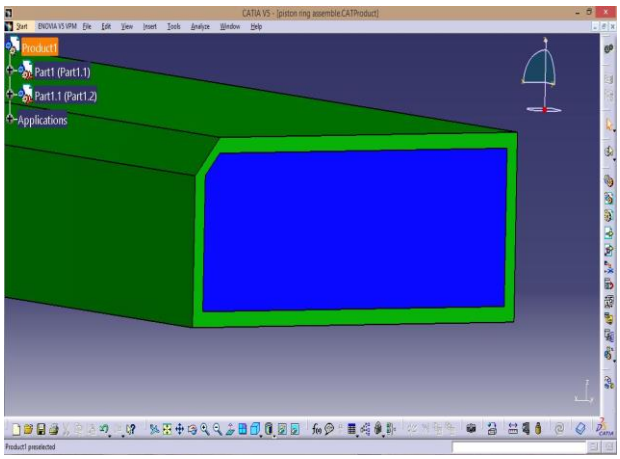

Fig. 7. CAD model of cross section of coated piston ring.

2.2.2 Finite element analysis of coated Piston ring

The finite element analysis for coating strength of piston ring is carried out using ANSYS classic version 14. Through such user interface various inputs are provided for analysis. The model is developed through a number of steps. The structural individual discipline is selected to show in the GUI with h-method. The preprocessing steps include creating the coated piston ring with required dimension in CATIA V5R19A or importing it to ANSYS as given in Figs. 8(a) and 8(b).

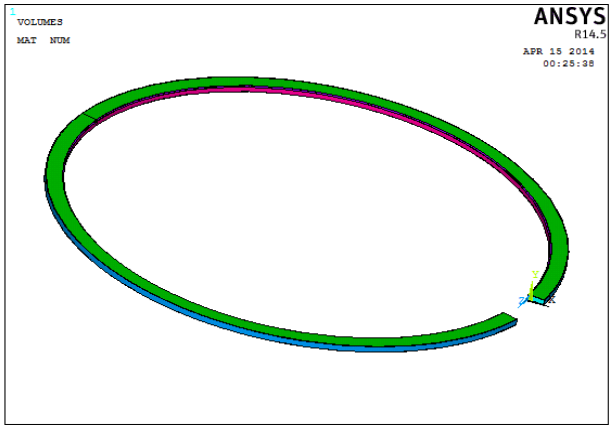

Fig. 8(a). Creating piston ring model (3 D).

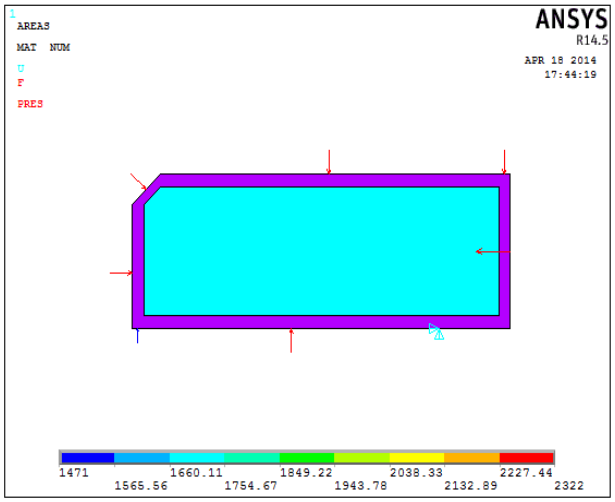

Fig. 8(b). Creating coated piston ring model (sectional view).

The element type was defined as SOLID-QUAD 4NODE 182 as shown in Figs. 9(a) and 9(b). Further, the material properties of the core and coating are defined. The core material is defined as steel, while coating material is as Nikasil.

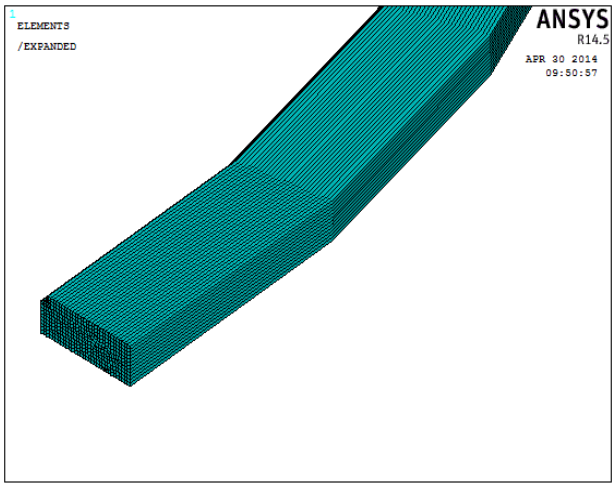

Fig. 9(a). Meshed view of enlarged piston ring.

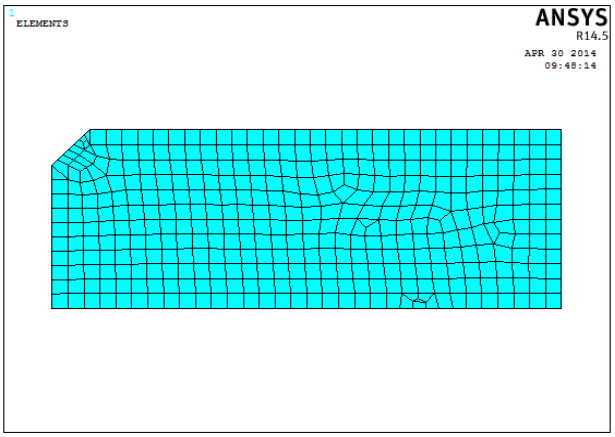

Fig. 9(b). Meshed view of cross section of piston ring.

Nikasil is short name for Nickel Silicon Carbide. Silicon carbide is a very hard ceramic (much harder than Steel) that can be dissolved in Nickel. The Nickel solution can then be electroplated onto the Aluminium cylinder bore. The piston rings will then rub off the exposed nickel, leaving a very hard layer of silicon carbide to protect the Aluminium piston from direct contact with the Aluminium cylinder. With this setup, the engine tolerances can be much tighter for better performance. The cylinder must be re-plated after it is re-bored, but Nikasil is extremely durable, so the cylinder does not need to be reworked as often as an iron or chrome cylinder do. Both, the core and the coating are isotropic material with material strength as stated in the Table 1.

Table 1. Material details of core and coating.

Component	Material	E (N/mm^2)	υ
Core	Steel	2.09x10^5	0.3
Coating	Nikasil	1.1x10^5	0.2

The next step is the meshing of the core and substrate. Meshing is a process to convert the whole geometry of the ring in to number of element. Such elements are connected by nodes. The model is meshed with QUADRILATERAL solid elements as shown in Fig. 9(a). For proper meshing, the smart size control on picked lines are set. Under element attribute, core area was set and the material was referred along with element type. Core area meshing is done using free quad shape. Similarly, the coating area was meshed using free quad as well. The mesh generated ring cross sectional area is given in Fig. 9(b). Loads that act in a ring during piston reciprocation are given in Fig. 6.

3. RESULT ANALYSIS

The forces defined in this case are at a crank location of highest gas pressure during piston upward motion/compression stroke. While in the downward stroke, the gas flow to the back of the ring is ceased. The Figure 10 represents the three dimensional view of loaded ring with different forces. The net deflection causes the ring to tilt vertically downward and is presented in Figs. 11 (a) and 11 (b) as per ring specification given in the Table 2.

Table 2. Ring specification.

Ring nominal diameter	82.2 mm
Axial width	2 mm
Moment of inertia	4.06 mm^4
Modulus of elasticity	203 *GPa*
Radius of neutral line: r_0 (mm)	39.7 mm
Tangential Force	10 N
Elastic pressure	0.20 *MPa*
Nominal Bore Diameter, mm	96 mm
Axial width	1 mm
Ring radial depth	3 mm
Modulus of elasticity	203 GPa
Poisson's ratio	0.23
Engine operating speed	13000 rpm
Lubricant dynamic viscosity at atmospheric pressure	0.004 Pas
Piezo-viscosity index	10^{-8} Pa^{-1}

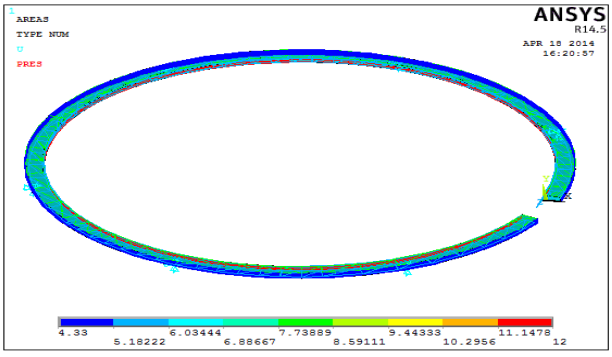

Fig. 10. Various forces acting on piston ring at highest gas pressure.

Due to the support on the lower groove land and application forces, the stress is developed on the ring surface and flows to the coating and substrate. In this analysis, the stress pattern is evaluated using von Misses failure criteria. In this case, the von Misses stress developed is presented in Fig. 12(a). The zone of the ring surface nearer to the point of contact with groove land is subjected to maximum stress. The Fig. 12(b) represents the 3-D volumetric strain calculated based on von-Misses criteria. The strain is maximum in the ring core and coating interface at the vicinity of the contact. The maximum value of von-Misses stress is 180.748 MPa as shown in Fig. 12(c), while that of the von-Misses strain is 0.004956, as shown in Fig. 12(d).

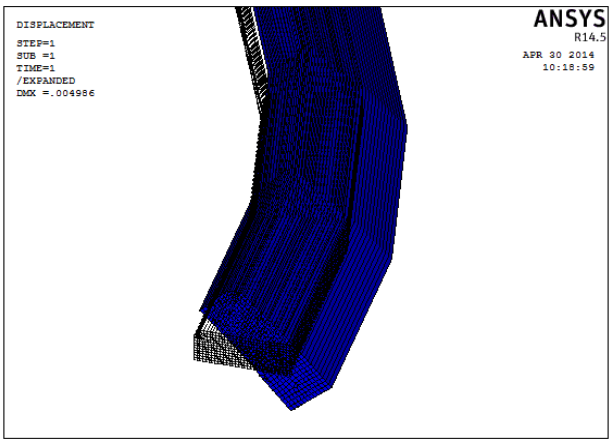

Fig. 11(a). Total deflection of 3-D meshed piston ring (enlarged view).

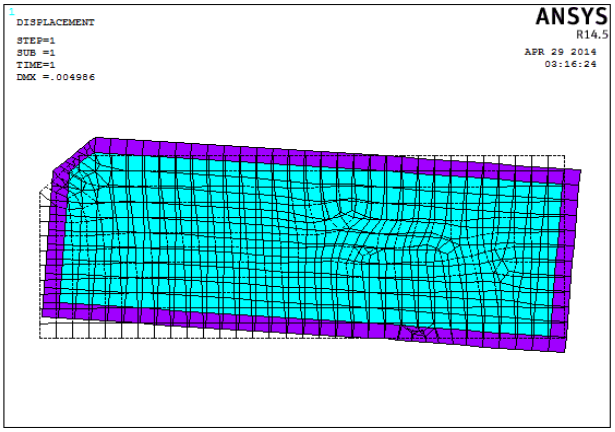

Fig. 11(b). Total deflection of meshed piston ring (cross sectional view).

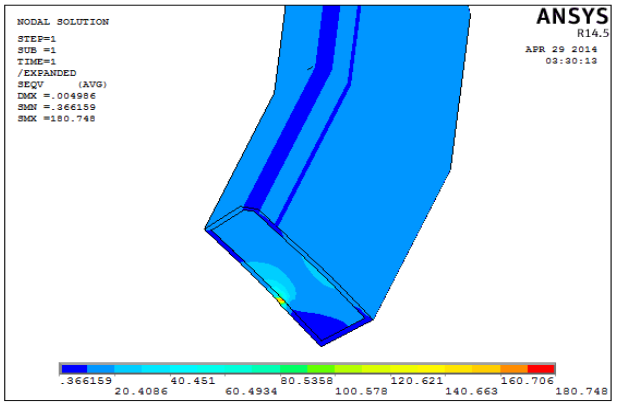

Fig. 12(a). von-Misses stress in 3-D meshed piston ring (enlarged view).

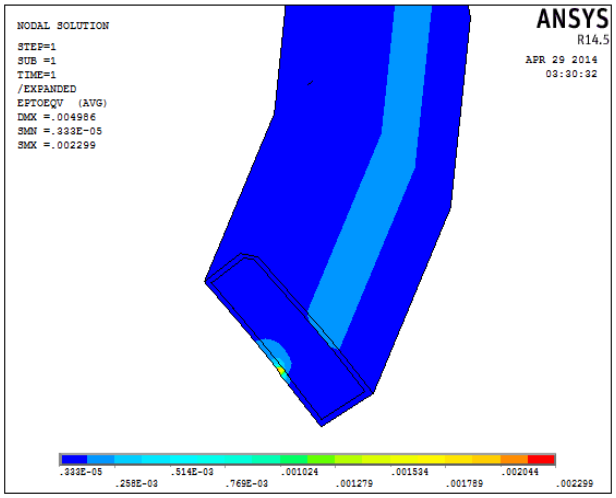

Fig. 12(b). von-Misses strain in 3-D meshed piston ring (enlarged view).

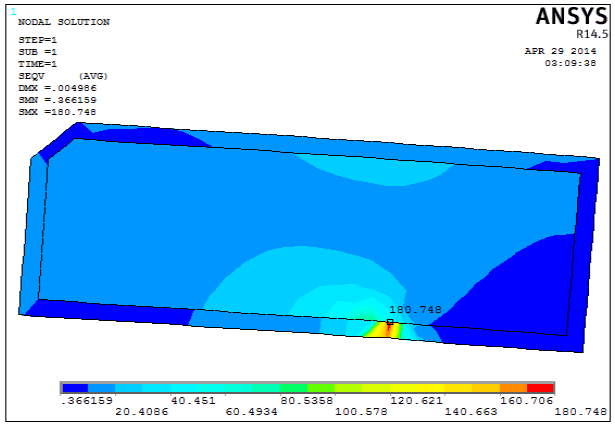

Fig. 12(c). Maximum von-Misses stress at the interface.

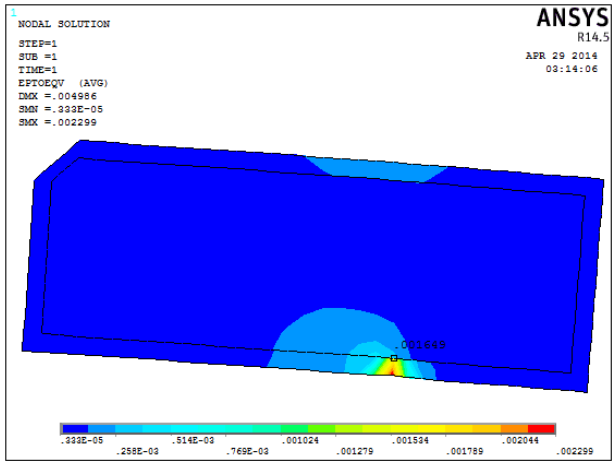

Fig. 12(d). Maximum von-Misses strain at the interface.

To understand the pattern of stress and strain in compression and power stroke, it is required to study the trends of same in different crank location with a series of combustion chamber pressure. It will help understand the cyclic nature of stress and strain. The Figure 13(a) represents the ring twist at 210^0, 240^0, 270^0 and 350^0 crank location respectively. The maximum deflection is around 3^0 about the horizontal axis. Similarly, the maximum von-Misses stress is 128 MPa at 350^0 crank location as stated in Fig. 13(b). The Figure 13(c) shows the von Misses strain upto 0.3 %.

During power stroke, the back pressure from the back of the ring ceased to flow. Hence the sealing action is produced by the ring elasticity alone. The Figures 14(a), 14(b) and 14(c) represent the deflection, von-Misses stress and von-Misses strain respectively on the power stroke. The fringe and magnitude of the parameters are different from that of compression stroke because of this reason.

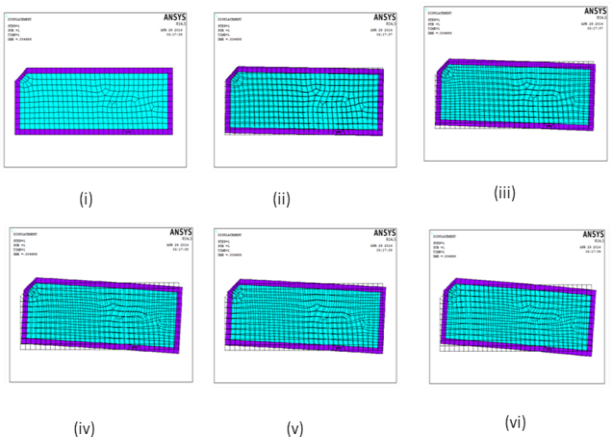

Fig. 13(a). Sequential tilting of ring due to deflection at different crank location during compression stroke.

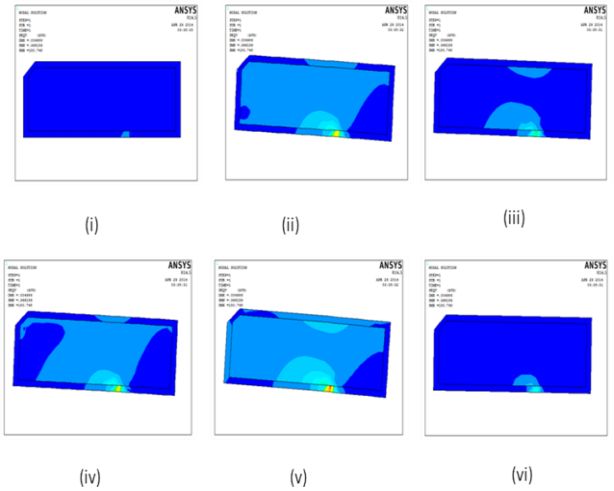

Fig. 13(b). Von-Misses stress fringe in coating and substrate interface during compression stroke.

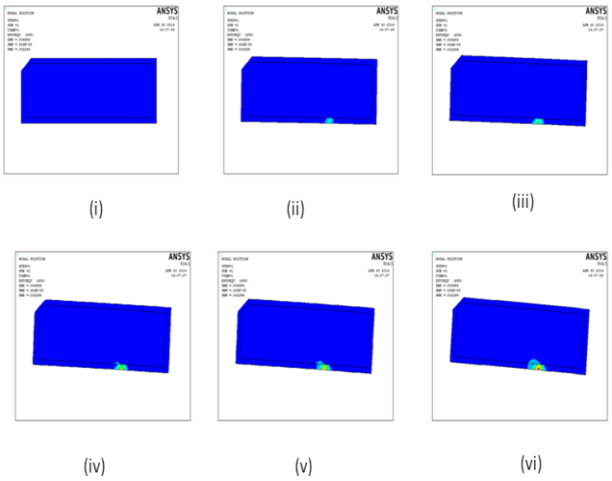

Fig. 13(c). Von-Misses strain fringe in coating and substrate interface during compression stroke.

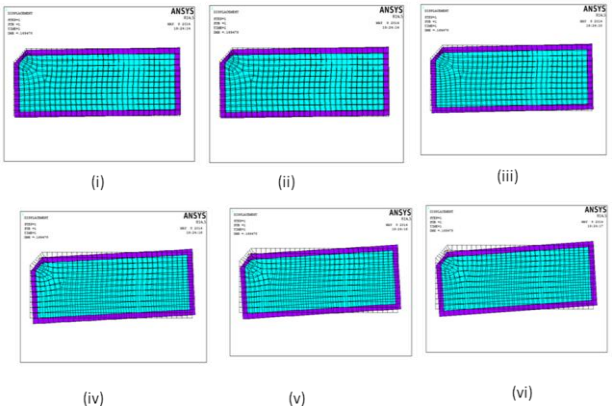

Fig. 14(a). Sequential tilting of ring due to deflection at different crank location during power stroke.

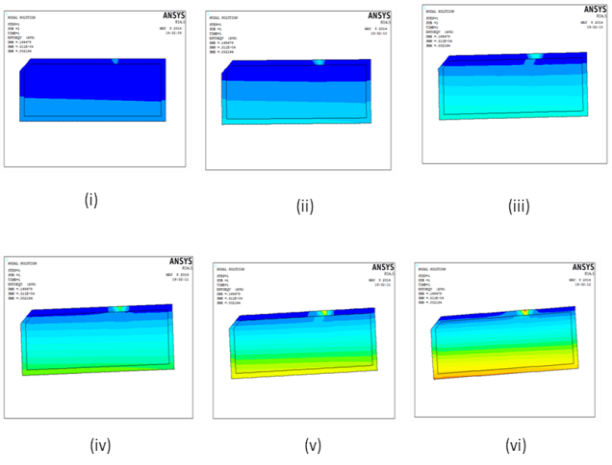

Fig. 14(b). Von-Misses stress fringe in coating and substrate interface during power stroke.

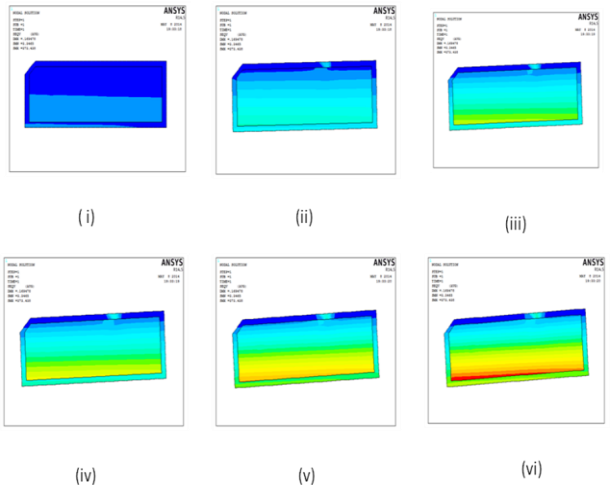

Fig. 14(c). von-Misses strain fringe in coating and substrate interface during power stroke.

4. CONCLUSION

The paper presented the co-relation between the tribodynamic issues and the coating substrate strength. The forces computed in addressing the former study are used as input to the FEM model. The highest tilting angle during compression ring is found to be 3^0 and the maximum von-Misses stress developed at the highest combustion chamber pressure is 128 MPa and much below the yield strength of the coating and the substrate. The strain calculated using von-Misses criteria is near to 0.3 %. Temperature stability analysis of coating in a rapid sliding environment in presence of elevated heat transfer will be a step further in this research.

Acknowledgement

We are very much thankful to the All India Council for Technical Education and Training (AICTE), New Delhi for funding this research. The funding of AICTE through RPS grant-in-aid to carry out our research project entitled “Advanced Engine Technology for Sustainable Development of Automotive Industry” is here acknowledged.

NOMENCLATURE

a	Ring depth	mm
b	Ring axial width	mm
A_i&B_i	Constant related to Fourier representation	
B_ψ	Parameter related gas blow by calculation	
C	Radial clearance	m
D	Diameter of the bore	mm
D_r	Nominal diameter of the fitted ring	m
E_c , E_r	Young's modulus for cylinder liner and piston ring	Nm^{-2}
E'	Apparent modulus of elasticity of the contacting pair	Nm^{-2}
F_e	Elastic pressure force	N
$F_g(\theta)$	Gas pressure force	N
F	Force due to hydrodynamic action	N
F_f	Fictional force due to hydrodynamic action	N
$F_{2.5}(\lambda_{rk})$	Probality distribution of asperity height	
$F_{ap}(F_e+F_g)$	Applied force in the ring due to combined action gas pressure and ring elasticity	N
F_{asp}	Asperity contact pressure	N
h_{sk} and h_r	Variable circumferential gap, Film thickness	μm
K^*	Constant used in calculation of asperity contact pressure	
N_a	Number of asperity per unit contact area	
p_{sk} , p_r	Hydrodynamic pressure	Mpa
P_1&P_2	Gas pressure at top and bottom of the ring	Mpa
R_b	Nominal bore radius	mm
$\Delta R(\theta)$	Bore radial difference	mm
t	Time	sec
U	Speed of entraining motion	ms^{-1}
U	Sliding velocity of the piston	ms^{-1}
W	Contact load (integrated pressure distribution)	N
x, y	Co-ordinate directions	
η& η_0	Lubricant dynamic viscosity and reference viscosity	Pas
$\xi_n(\theta)$	Conformability	
$K(x)$	Undeformed axial ring profile	μm
ρ	Lubricant density	Kgm^{-3}
τ	Total Shear stress	Nm^{-2}
θ	Crank location in degree	m
Φ_p	Pressure flow factor	
Φ_s	Shape flow factor	
$(\Phi_{fg}, \Phi_{fp}, \Phi_{fs})$	Flow factors used for friction calulation	
$\delta(x, \theta)$	Ring global deformation	m
Δ_b	Ring off set	m
β^*	Asperity tip radius	m
υ	Damping factor	
$\begin{pmatrix}\phi_p,\phi_s,\\ \phi_g,\phi_{fg},\\ \phi_{fp}\phi_{fs}\end{pmatrix}$	Flow factors of geometry, pressure and shear	
λ_{rk}	Stribeck's oil film parameter	-

REFERENCE

[1] T. Tian, 'Dynamic behaviours of piston rings and their practical impact. Part 1: ring flutter and ring collapse and their effects on gas flow and oil transport', *Proceedings of the Institution of Mechanical Engineers, Part J: Journal of Engineering Tribology*, vol. 216, no. 4, pp. 209-228, 2002.

[2] T. Tian, 'Dynamic behaviours of piston rings and their practical impact. Part 2: oil transport, friction and wear of ring/liner interface and the effects of piston and ring dynamics', *Proceedings of the Institution of Mechanical Engineers, Part J: Journal of Engineering Tribology*, vol. 216, no. 4, pp. 229-248, 2002.

[3] S. Kurbet and R. Kumar, 'A finite element study of piston tilt effects on piston ring dynamics in internal combustion engines', *Proceedings of the Institution of Mechanical Engineers, Part K: Journal of Multi-body Dynamics*, vol. 218, no. 2, pp. 107-117, 2004.

[4] V.V. Dunaevsky, S. Alexandrov and F. Barlat, 'Analysis of Three-Dimensional Distortions of the Piston Rings with Arbitrary Cross-Section', *SAE Technical Paper*, no.2000-01-3453, pp. 1-7, 2000.

[5] A.A. Minewitsch, 'Some developments in triboanalysis of coated machine components', *Tribology in Industry*, vol. 33, no. 4, pp. 153-158, 2011.

[6] M. Urgen, 'Production and Characterization of MeN-X type Nanocomposite coatings produced by cathodic arc based hybrid technique', in *International Surface Engineering Congress and Exhibition*, August 2-4, Orlando, FI USA, 2004.

[7] M. Okamoto and I. Sakai, 'Contact Pressure Distribution of Piston Rings -Calculation based on Piston Ring Contour', *SAE Technical Paper*, 2001-01-0571, pp. 1-7, 2001.

[8] S. Timoshenko, *Elementary Theories and Problems*. D. Van Nostrand Co, New York, 1955.

[9] P.C. Mishra, 'Tribodynamic modeling of piston compression ring cylinder liner contact at high pressure zone of engine cycle', *International Journal of Advances in Manufacturing Technology*, vol. 66, no. 5-8, pp. 1075-1085, 2013.

[10] M. Hlaváček, 'A central film thickness formula for elastohydrodynamic lubrication of cylinders with soft incompressible coatings and a non-Newtonian piecewise power-law lubricant in steady rolling motion', *Wear*, vol. 205, no. 1-2, pp. 20-27, 1997.

[11] M. Tanaka, Y. Kitajima, Y. Endoh, M. Watanabe and Y. Nagita, 'Ceramic-metal Composite Coated Piston Ring and Cylinder Liner of Marine Low Speed Diesel Engine', *Journal of the MESJ*, vol. 27, no. 3, pp. 238-247, 1992.

[12] F. Funatani and K. Kurosawa, 'Improved engine performance via use of Nickle Ceramic composite', *SAE Technical Paper,* no.940852*,* pp. 89-96, 1994.

[13] M. Kennedy, S. Hoppe and J. Esser, 'Piston Ring Coating Reduces Gasoline Engine Friction', *MTZ Worldw*, vol. 73, no. 5, pp. 40-43, 2012.

[14] S. Tung and M. McMillan, 'Automotive tribology overview of current advances and challenges for the future', *Tribology International*, vol. 37, no. 7, pp. 517-536, 2004.

[15] K.D. Bouzakis, M. Pappa, S. Gerardis, G. Skordaris, E. Bouzakis, 'PVD coating strength properties at various temperatures by Nano indentation and FEM calculation', *Tribology in Industry*, vol. 34, no. 1, pp. 29-34, 2012.

[16] D. Barrell, M. Priest and C. Taylor, 'Experimental simulation of impact and sliding wear in the top piston ring groove of a gasoline engine', *Proceedings of the Institution of Mechanical Engineers, Part J: Journal of Engineering Tribology*, vol. 218, no. 3, pp. 173-183, 2004.

[17] P.C. Mishra, H. Rahnejat and P.D. King, *Tribology of piston compression ring*. Woodhead publishing, Cambridge, UK, 2010.

[18] P.C. Mishra, 'Modelling for friction of four stroke four cylinder petrol engine', *Tribology in Industry*, vol. 35, no. 3, pp. 237-245, 2013.